EXHIBIT 2

4. B. Julesz, *Foundations of Cyclopean Perception* (Univ. of Chicago Press, Chicago, 1971).
5. Borrowing ideas from information theory [C. E. Shannon and W. Weaver, *The Mathematical Theory of Communication* (Univ. of Illinois Press, Urbana, IL, 1949); W. R. Garner, *Uncertainty and Structure as Psychological Concepts* (Wiley, New York, 1962)], we can characterize a series of signals over time as an ensemble of n distinct messages ($m_1, m_2 \ldots m_i \ldots m_n$) whose individual probabilities ($p_1, p_2 \ldots p_i \ldots p_n$) sum to unity. Then the information (expressed in binary units: bits) conveyed by each message is given by

$$H_i = -\log_2(p_i)$$

and the average information associated with the entire ensemble of messages is given by

$$H_w = -\Sigma_{i=1}^{n} p_i * \log_2(p_i)$$

Although not widely used in work in visual perception, the concept of entropy has been successfully applied in the study of human stereopsis [B. Julesz and C. W. Tyler, *Biol. Cybern.* **23**, 25 (1976)] and motion perception [D. Gilden, E. Hiris, R. Blake, *Psychol. Sci.* **6**, 235 (1995)].
6. D. R. Brillinger, *Can. J. Stat.* **22**, 177 (1994); R.-D. Reiss, *A Course on Point Process* (Springer-Verlag, New York, 1993).
7. Gray-scale animations were created on a NEC 21-inch monitor (frame rate 100 Hz; pixel resolution 1024 vertical by 768 horizontal; P104 phosphor) using MatLab in conjunction with the Psychophysics toolbox [D. Brainard, *Spat. Vision* **10**, 443 (1997)]; all display and trial-related events were programmed on a Macintosh Power PC computer. Luminance nonlinearities were corrected using a calibrated look-up table. The display consisted of 676 Gabor elements regularly arrayed within a 6.7° by 6.7° square (average luminance 24.5 cd/m²). Individual Gabor elements did not overlap visually within the array. Each Gabor patch was the product of a sinusoidal grating and a circular Gaussian envelope with a standard deviation of ±4.5 arc min. The peak spatial frequency of every grating was 5.8 cycles per degree (bandwidth 1.2 octaves), the contrast of every grating was 0.80, and the orientation of each grating was randomly set. Each grating moved at 3.45° per second in one of two directions orthogonal to its orientation, with smooth apparent motion being produced by phase-shifting the grating from frame to frame of the animation by one-fifth of the grating cycle synchronized to the monitor frame rate. The direction of motion of each grating within the stationary window reversed over time unpredictably according to the Poisson distribution. New animations were created and stored on hard disk before each test session. Demonstrations of these displays can be seen at http://www.psy.vanderbilt.edu/faculty/blake/Demos/TS/TS.html.
8. One of the principles of perceptual organization identified by Gestalt psychologists was common fate, a form of temporal structure in which visual elements moving in the same direction appear to group into a single object. Birds flying in the same direction, for example, perceptually form a global unit called a flock.
9. D. Regan and S. Hamstra, *Perception* **20**, 315 (1991).
10. Each stimulus element in this display consisted of a radial grating 19 arc min in diameter. Each grating resembled a circular "windmill" divided into four equal-sized wedges, two black and two white. The starting phase of each windmill was random. When animated, each windmill rotated 45° (1/2 wedge size) from frame to frame, producing smooth apparent rotation whose direction was unambiguous. Average luminance of the display was 24.5 cd/m². For the stereoscopic experiment involving presentation of two windmill arrays, each array consisted of 324 windmills within a 5.8° by 5.8° square. Each array contained two virtual "figure" regions, each 1.9° (horizontal) by 1.3° (vertical) on a side, located immediately above and below a small, central fixation mark. Crossed disparity was introduced into the upper pair of figures or the lower pair of figures by shifting the corresponding "figure" regions 1 windmill diameter to the left in one eye and 1 diameter to the right in the other eye; this produced an effective disparity of 38.6 arc min. For this experiment, rotational reversals of windmills defining the background region of the two half-images followed one point process, reversals of windmills defining the upper pair of "figures" in the two half-images followed another point process, and the reversals for the lower pair of "figures" followed a third point process.
11. In preliminary work we also found that synchronized, irregular changes in luminance can promote spatial grouping [S.-H. Lee and R. Blake, *Invest. Ophthalmol. Visual Sci.* **40**, S45 (1999)]; S. E. Palmer (paper presented at the 39th annual meeting of the Psychonomic Society, Dallas, TX, 21 November 1998) found that periodic, synchronized changes in size, shape, or color can bias perceptual organization.
12. D. Regan, *Vision Res.* **29**, 1389 (1989); S. Anstis and V. S. Ramachandran, in *The Artful Eye*, R. Gregory, J. Harris, P. Heard, D. Rose, Eds. (Oxford Univ. Press, New York, 1995), p. 232; M. Bravo and R. Blake, *Vision Res.* **32**, 1793 (1992); D. J. Field, A. Hayes, R. F. Hess, *ibid.* **33**, 173 (1993).
13. I. Biederman, *Psychol. Rev.* **94**, 115 (1987); M. C. Mozer, *The Perception of Multiple Objects: A Connectionist Approach* (MIT Press, Cambridge, MA, 1991); S. Grossberg, *Neural Networks* **6**, 463 (1993); S. P. Vecera and R. C. O'Reilly, *J. Exp. Psychol. Hum. Percept. Perform.* **24**, 441 (1998).
14. Models of structure from motion extract discontinuities—boundaries—within a field of local motion vectors, with grouping based on common directions or speeds of motion [N. M. Grzywacz, S. N. J. Watamaniuk, S. McKee, *Vision Res.* **35**, 3183 (1995); W. B. Thompson, D. Kersten, W. R. Knecht, *Biol. Cybern.* **66**, 327 (1992); J. Chey, S. Grossberg, E. Mingolla, *J. Opt. Soc. Am. A* **14**, 2570 (1997)]. In our displays, motion direction is completely random throughout the array of elements. Speed too is constant except at the moment of reversal. It is conceivable that reversals in motion direction create brief transients in speed-selective neurons, which could constitute the neural embodiment of the point processes defining temporal structure (Fig. 1C).
15. C. Chubb and G. Sperling, *J. Opt. Soc. Am. A* **5**, 1986 (1988); H. R. Wilson and J. Kim, *Vis. Neurosci.* **11**, 1205 (1994); P. Cavanagh, *Science* **257**, 1563 (1992); Z.-L. Lu and G. Sperling, *Nature* **377**, 237 (1995).
16. Supported by NIH grants EY07760 and EY01826. We thank J. Schall, A. B. Bonds, M. Donnelly, S. Grossberg, W. Newsome, and J. Lappin for helpful discussions.

1 February 1999; accepted 7 April 1999

Bone Marrow as a Potential Source of Hepatic Oval Cells

B. E. Petersen,[1]* W. C. Bowen,[1] K. D. Patrene,[2] W. M. Mars,[1] A. K. Sullivan,[4]† N. Murase,[3] S. S. Boggs,[2] J. S. Greenberger,[2] J. P. Goff[2]

Bone marrow stem cells develop into hematopoietic and mesenchymal lineages but have not been known to participate in production of hepatocytes, biliary cells, or oval cells during liver regeneration. Cross-sex or cross-strain bone marrow and whole liver transplantation were used to trace the origin of the repopulating liver cells. Transplanted rats were treated with 2-acetylaminofluorene, to block hepatocyte proliferation, and then hepatic injury, to induce oval cell proliferation. Markers for Y chromosome, dipeptidyl peptidase IV enzyme, and L21-6 antigen were used to identify liver cells of bone marrow origin. From these cells, a proportion of the regenerated hepatic cells were shown to be donor-derived. Thus, a stem cell associated with the bone marrow has epithelial cell lineage capability.

Hepatic oval cells proliferate under certain conditions, mainly when hepatocytes are prevented from proliferating in response to liver damage, and may be stem cells for hepatocytes and bile duct cells or the intermediate progeny of a hepatic stem cell. Oval cells may originate either from cells present in the canals of Herring (*1*) or from blastlike cells located next to bile ducts (*2*). Oval cells have been shown to proliferate in certain pathological conditions, in which hepatocyte proliferation is inhibited before severe hepatic injury. In experimental models, hepatocyte proliferation is suppressed by exposure of the animal to 2-acetylaminofluorene (2-AAF), and hepatic injury can be induced by partial hepatectomy or by administration of carbon tetrachloride (CCl_4) (*3*, *4*). Oval cells express CD34, Thy-1, and c-kit mRNAs and proteins (*5*–*7*) and flt-3 receptor mRNA (*8*), all of which are also found in hematopoietic stem cells (HSC).

We tested the hypothesis that oval cells and other liver cells may arise from a cell population originating in, or associated with, the bone marrow (BM). This hypothesis was tested by three approaches: (i) bone marrow transplantation (BMTx) from male rats into lethally irradiated syngeneic females and detection of donor cells in the recipients by means of DNA probes to the Y chromosome *sry* region; (ii) BMTx from dipeptidyl peptidase IV–positive (DPPIV⁺) male rats into DPPIV⁻ syngeneic females and detection of

[1]Department of Pathology, [2]Department of Radiation Oncology, [3]Division of Transplant Pathology, Department of Pathology, School of Medicine, University of Pittsburgh, Pittsburgh, PA 15261, USA. [4]Department of Hematology/Oncology, McGill University, Quebec H3A 2T5, Canada.

*To whom correspondence should be addressed. E-mail: bryon+@pitt.edu

†Present address: Department of Oncology, King Faisal Specialist Hospital and Research Centre, Post Office Box 3354, Riyadh, Kingdom of Saudi Arabia.

DPPIV-expressing cells in the recipient animals; and (iii) whole liver transplantation (WLTx) with Lewis rats that express the L21-6 antigen as recipients and Brown-Norway rats that do not express this antigen as allogeneic donors (*9*) to confirm that an extrahepatic source (L21-6$^+$ cells) could repopulate the transplanted (L21-6$^-$ cells) liver. In conjunction with these approaches, the 2-AAF–CCl_4 protocol (*4*, *5*) was used to induce oval cell activation and proliferation. In situ hybridization, polymerase chain reaction (PCR), and immunocytochemistry were used to distinguish donor cells from recipient cells.

Female rats were lethally irradiated and rescued with a BM transplant from a male animal. Nucleated blood cells of the transplanted animals were tested by PCR to establish that the BMTx was successful (*10*). Engrafted females were then placed on the oval cell protocol (*4*, *5*). Both Thy-1$^+$ and Thy-1$^-$ cell populations of nonparenchymal cells (NPC) from days 9 and 13 after hepatic injury were positive for the Y chromosome PCR product (Fig. 1). The strong signal from the Thy-1$^-$ fraction was probably due to donor hematopoietic cells that are in the NPC population and Thy-1$^-$ but are positive for the Y chromosome. The day 9 hepatocyte fraction had no Y chromosome signal, but by day 13 a signal from the hepatocyte fraction was detected. At this time, the oval cells are beginning to differentiate into hepatocytes (*1*). If all oval cells that differentiate into hepatocytes were derived from the liver, then one would expect that none of the hepatocytes tested would be positive for the Y chromosome. The finding that some hepatocytes were Y chromosome–positive suggests that they were derived from the BM donor cells. The combined data suggest that at day 9 the oval cells (Thy-1$^+$) (*5*) in the recipient female are derived from the donor male and that they continue to differentiate into mature hepatocytes by day 13.

To confirm the PCR results, we performed in situ hybridization for the Y chromosome *sry* gene on frozen sections (*11*). Hepatocytes carrying a positive reaction product (blue staining) in the nuclei were seen in untreated control male rats (Fig. 2A). In agreement with the results obtained by PCR analyses of the isolated hepatocyte frac-

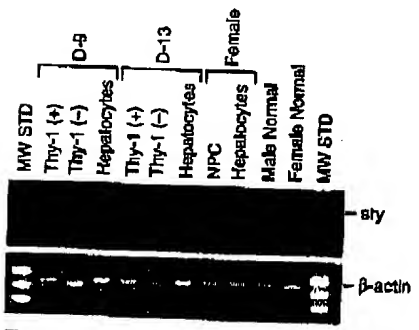

Fig. 1. PCR analyses of DNA from female rats transplanted with BM from male donor rats. Primers for the *sry* gene were used (*10*). *sry* expression is seen in hepatocytes at day 13 after the 2-AAF–CCl_4 protocol from donor-derived cells. No expression is seen in females. The data presented are representative of four independent experiments. MW STD, molecular weight standard; D-9, day 9; D-13, day 13. β-actin was used as control.

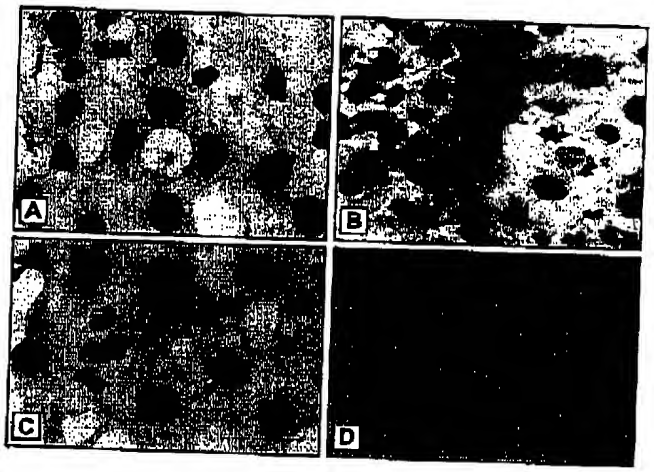

Fig. 2. In situ hybridizations of the Y chromosome *sry* gene on frozen liver sections. Arrows indicate positive signals in the nuclei of cells. (A) Untreated normal male rat control. (B and C) Female rats treated with BMTx and the 2-AFF–CCl_4 protocol and killed at day 9 (B) and day 13 (C) after hepatic injury. (D) Untreated female (negative control). Scale bar, 15 μm.

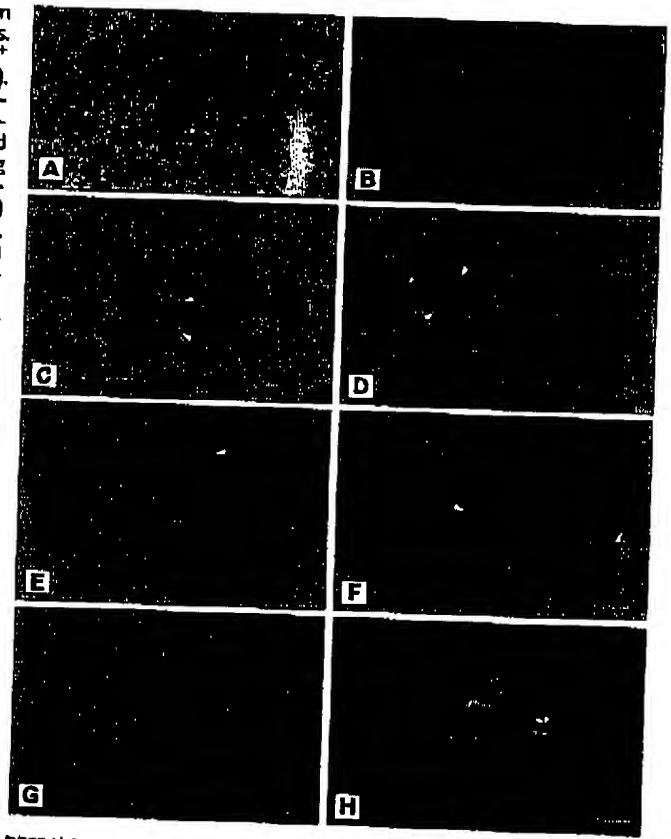

Fig. 3. DPPIV activity in frozen liver sections. (A) Untreated DPPIV$^+$ rat (positive control). DPPIV staining is evident (red-orange color). (B) Untreated DPPIV$^-$ rat showing absence of DPPIV (negative control). (C to F) Four different BMTx. Male DPPIV$^+$ (donor) or female DPPIV$^-$ (recipient) rats were exposed to the 2-AAF–CCl_4 protocol for oval cell induction and killed at day 11 or 13 after hepatic injury. A positive reaction is evident between hepatocytes from all four animals and on a few oval or transitional cells (E). DPPIV staining appears as a line (open arrowheads) or dot (closed arrowheads) depending on the plane of the section through the bile canalicular region. In all cases, there are clusters of cells expressing DPPIV. The asterisks indicate donor origin hepatocytes. (G) Control DPPIV$^-$ female after BMTx but before 2-AAF–CCl_4 protocol. No DPPIV$^+$ hepatocytes were observed; an occasional DPPIV$^+$ hematopoietic cell was seen (arrowhead). (H) Immunofluorescent staining of mature hepatocytes, after transplantation and 2-AAF–CCl_4 protocol. Three markers were used: DPPIV–Texas Red, H4-AMCA (stains the cytoplasm of mature hepatocytes), and C-CAM-FITC (a hepatocyte-specific cell adhesion molecule). In the bile canalicular region, the blue cells (H4 positive), which are also are positive for both DPPIV and C-CAM, appear yellow. Scale bars, 60 μm (F) and 30 μm (H).

tion, cells with positive signal (Y chromosome) were detected in oval cells of females subjected to BMTx and 2-AAF–CCl_4 at both days 9 (Fig. 2B) and 13 and hepatocytes at day 13 (Fig. 2C). No signal was detected in the liver of an untreated control female (Fig. 2D). In 100 random fields, about 0.14% of the total hepatocytes were positive for the Y chromosome. Therefore, about 9.9×10^5 hepatocytes originated from transplanted BM cells on day 13 after hepatic injury. In addition, the proportion of Thy-1^+ oval cells expressing the Y marker was about 0.1% (*12*).

In an independent approach, BM cells from DPPIV$^+$ F-344 male rats were injected into lethally irradiated DPPIV$^-$ F-344 females, and the recipients were treated with the 2-AAF–CCl_4 protocol. This constituted a system in which the presence of cells originating from donor cells in the recipient liver could be easily detected, by revealing cytochemically the activity of the enzyme DPPIV (Fig. 3). A diffuse red to red-orange staining of the bile canalicular site between hepatocytes (*13*) was observed in the DPPIV$^+$ F-344 male rats (Fig. 3A). The control untreated DPPIV$^-$ females showed no staining (Fig. 3B). DPPIV expression was observed in a number of bile canalicular sites between hepatocytes from several different transplanted animals (Fig. 3, C to F). DPPIV expression was also observed on oval cells and transitional (small hepatocyte) cells in the liver from these rats (Fig. 3, D and E). Out of 250 random fields, about 0.16% of the hepatocytes were positive for DPPIV. Therefore, about 1.0×10^6 hepatocytes originated from transplanted BM cells by day 13 after hepatic injury (*12*). In control DDPIV$^-$ females, no DPPIV$^+$ hepatocytes were observed after BMTx but before 2-AAF–CCl_4 (Fig. 3G). To demonstrate that the donor-derived hepatocytes were mature, we performed three-color immunofluorescence. DPPIV$^+$ hepatocytes also stained positive for the mature hepatocyte-specific markers, H4 and C-CAM (Fig. 3H) (*14*). This result shows definitively that the cells are mature hepatocytes (H4- and C-CAM–positive) that have been integrated into the parenchyma and are carrying the transplant marker (DPPIV$^+$).

Our final approach to examine extrahepatic cells repopulating the liver was WLTx. Lewis rats that express the major histocompatibility complex class II L21-6 isozyme were recipients of liver from Brown-Norway rats that do not express L21-6 (*15*). A monoclonal antibody to L21-6 differentiated donor from recipient cells. Oval cells that originated from an extrahepatic source would be L21-6–positive, whereas those originating in situ would be negative. Brown-Norway rat livers transplanted into Lewis rats after the 2-AAF–CCl_4 protocol show a widespread staining of L21-6 in the transplanted Brown-Norway livers, a result of the influx of Lewis immune cells reacting to the allogeneic Brown-Norway liver. Ductal structures also contained L21-6–positive cells in a pattern often seen in the organization and differentiation of actively proliferating oval cells (*16, 17*), indicating that some oval cells were derived from an extrahepatic source and others, L21-6–negative, were derived in situ from the donor liver (*18*).

Under specific physio-pathological conditions, oval cells can differentiate into the two types of epithelial cells present in the liver: ductular cells and hepatocytes (*1, 16, 17*). Oval cells may have a role in the genesis of chemically induced hepatocellular carcinomas, but they also have a potential use in the therapy of acute liver failure syndromes. Oval cell precursors are thought to be located either in the canals of Herring or next to the bile ducts (*1, 2*). Ductal epithelium is required for oval cell proliferation (*19*), indicating that either it is the source of the precursors or it acts in a supportive or inductive role. Oval cells have some phenotypic traits that are typical of BM stem cells (*5–8*). The liver harbors many hematopoietic cell types, including HSC (*20*), and if oval cells could originate from either BM-derived cells or self-replication, one would expect to see a subpopulation of negative oval cells from resident cells in the liver of Brown-Norway rats, as well as a population of positive cells originating from cells that migrated into the liver from the L21-6–positive host. Our Brown-Norway into Lewis liver transplant data support this hypothesis (*18*).

Our data lend credence to the possibility that a cell associated with the BM may act, under certain physio-pathological conditions, as the progenitor of several types of liver cells. The limits and biological importance of these BM-derived cells need to be assessed; the BM-derived cells add to the growing body of evidence suggesting that cells in the adult organism have a remarkable degree of plasticity (*21–23*).

References and Notes

1. J. W. Grisham and S. S. Thorgeirsson, in *Stem Cells*, C. S. Potten, Ed. (Academic Press, San Diego, CA, 1997), chap. 8.
2. P. M. Novikoff, A. Yam, I. Oikawa, *Am. J. Pathol.* 148, 1473 (1996).
3. R. P. Evarts, P. Nagy, H. Nakatsukas, E. Marsden, S. S. Thorgeirsson, *Cancer Res.* 49, 1541 (1989).
4. B. E. Petersen, V. F. Zajac, G. K. Michalopoulos, *Hepatology* 27, 1030 (1998).
5. B. E. Petersen, J. P. Goff, J. S. Greenberger, G. K. Michalopoulos, *Ibid.*, p. 433.
6. N. Omori *et al.*, *Ibid.* 26, 720 (1997).
7. K. Fujio, R. P. Evarts, Z. Hu, E. R. Marsden, S. S. Thorgeirsson, *Lab. Invest.* 70, 511 (1994).
8. M. Omori, N. Omori, R. P. Evarts, T. Teramoto, S. S. Thorgeirsson, *Am. J. Pathol.* 150, 1179 (1997).
9. BMTx was done as described [N. Murase *et al.*, *Transplantation* 61, 1 (1996)]. In two separate experiments, BM from male F-344 rats was transplanted into lethally irradiated syngeneic female F-344 rats (n = 10 animals) (F-344 male and female rats from Frederick Labs, Frederick, MD). To test if donor cells had engrafted, we performed PCR analysis on DNA extracted from the buffy coat of nucleated cells obtained from retinal orbital blood. Transplant survival was 100%, and varying degrees of chimerism were observed. Only animals expressing a strong signal for the Y chromosome PCR product were placed on the 2-AAF–CCl_4 protocol. Animals were killed 9 to 13 days after CCl_4 administration. In a second set of BMTx experiments, BM from male F-344 rats expressing the DPPIV enzyme was transplanted into lethally irradiated DPPIV$^-$ syngeneic female F-344 rats (n = 14 animals) and then treated as above. WLTx was performed as described [N. Murase *et al.*, *Transplantation* 60, 158 (1995)].
10. PCR analysis for the Y chromosome was done on DNA extracted from transplanted and nontransplanted female animals with primers for the *sry* gene of the Y chromosome [J. An, V. N. Beauchemin, J. Albanese, A. K. Sullivan, *J. Androl.* 18, 289 (1997)].
11. In situ hybridization of the *sry* region of the Y chromosome was performed with digoxigenin-labeled DNA probes (Boehringer Mannheim) hybridized to frozen liver sections.
12. An estimate of the number of hepatocytes originating from the donor BM (Y chromosome–positive hepatocytes in BMTx females and DPPIV-positive hepatocytes in BMTx DPPIV-deficient females) was determined from animals showing the strongest evidence of donor marrow engraftment, based on examination of the recipient's spleens (n = 4 animals for each model). In each of the BMTx DPPIV-deficient females, 10 sections per lobe were cut from five lobes (50 sections total) and stained, and 25 random fields per section were examined (250 total per animal) for DPPIV-positive hepatocytes. Rat liver has about 700×10^6 hepatocytes; this value was used to calculate the number of hepatocytes that originated from transplanted BM cells on day 13 after hepatic injury. For the percentage of Y chromosome–positive hepatocytes in BMTx females, five sections per lobe were cut from three lobes (15 sections total); after in situ hybridization, 20 random fields per section (100 total per animal) were examined for Y chromosome–positive hepatocytes. The percentage of Thy-1^+ oval cells expressing the Y marker was calculated from in situ hybridization cytospin preparation from four different animals.
13. For immunocytochemistry, tissue was placed in optimum cutting temperature compound (O.C.T.) and cold 2-methylbutane and processed for frozen sections. DPPIV activity was detected with the cytochemical method of Z. Lojda [*Histochemistry* 57, 107 (1979)].
14. D. C. Hixson, R. A. Farris, L. Yang, P. Novikoff, in *The Role of Cell Types in Hepatocarcinogenesis*, A. E. Sirica, Ed. (CRC, Ann Arbor, MI, 1992), chap. 8.
15. A Yagihashi *et al.*, *Transplant. Proc.* 27, 1519 (1995).
16. S. S. Thorgeirsson, R. P. Evarts, H. C. Bisgaard, K. Fujio, Z. Hu, *Proc. Soc. Exp. Biol. Med.* 204, 253 (1993).
17. N. Fausto, in *The Liver: Biology and Pathobiology*, I. M. Arias *et al.*, Eds. (Raven, New York, ed. 3, 1994), chap. 78.
18. Brown-Norway rat livers were transplanted into Lewis recipient rats (n = 6) (9). The four surviving rats were killed 11 and 13 days after the 2-AAF–CCl_4 oval cell induction protocol. A portion of the cells in the periportal region were positive for both L21-6-FITC and OC-2-Texas Red (an oval cell and mature ductal cell marker) by immunofluorescence.
19. B. E. Petersen, V. F. Zajac, G. K. Michalopoulos, *Am. J. Pathol.* 151, 905 (1997).
20. H. Taniguchi, T. Toyoshima, K. Fukao, H. Nakauchi, *Nature Med.* 2, 198 (1996).
21. C. Hagios, A. Lochter, M. J. Bissell, *Philos. Trans. R. Soc. London B Biol. Sci.* 353, 857 (1998).
22. G. Ferrari *et al.*, *Science* 279, 1528 (1998).
23. T. Asahara *et al.*, *Ibid.* 275, 964 (1997).

24. We thank L. Shab, J. Kalfs, and R. Dravian for help with the figures; B. Lombardi, P. Lindroos, D. Beer-Stolz, and M. Molitor for review of the manuscript; S. Gupta for DPPIV$^-$ female F-344 rats; and R. Farris and D. Hixson for antibodies.

17 November 1998; accepted 16 April 1999